Energy dependence of the total reaction cross section of isomeric $^{18}F^m$ on silicon below 400 MeV

D. A. Roberts, F. D. Becchetti, J. Jänecke, M. Y. Lee, T. W. O'Donnell, and K. Pham
Department of Physics, University of Michigan, Ann Arbor, Michigan 48109

J. A. Brown
Department of Physics, Millikin University, Decatur, Illinois 62522

R. E. Warner
Department of Physics, Oberlin College, Oberlin, Ohio 44074

R. M. Ronningen
National Superconducting Cyclotron Laboratory, Michigan State University, East Lansing, Michigan 48824

H. W. Wilschut
Kernfysisch Versneller Instituut, Zernikelaan 25, 9747 AA Groningen, The Netherlands
(Received 1 October 2001; published 19 March 2002)

A 25 MeV/nucleon primary ^{17}O beam was used to produce an isomeric state $^{18}F^m$ beam via the single-nucleon transfer reaction ^{17}O (^{12}C, ^{11}B) $^{18}F^m$. The total nuclear reaction cross section, σ_R, of $^{18}F^m$ (metastable) on silicon was measured using a stack of silicon surface barrier detectors that included a position sensitive silicon detector (PSD). The total reaction cross sections were determined as a function of bombarding energy up to 400 MeV by measuring the energy loss in each detector. The reaction cross sections were measured both for a mixture of metastable- and ground-state ions and for a pure ground-state beam. The reaction cross sections for ^{14}N and ^{16}O beams were also measured simultaneously. The reaction cross sections for the metastable beam were deduced from the mixed- and the ground-state cross sections, corrected for the measured purity of the mixed-state beam. The observed reaction cross sections for $^{18}F^m$ are larger at low energies than the cross sections measured for the ground state. The isomeric cross sections can be reproduced by an optical model potential having a diffuseness of 0.8 fm, compared to a more conventional diffuseness parameter of 0.5 fm, which is adequate to reproduce the ^{14}N, ^{16}O, and $^{18}F_{g.s.}$ cross sections measured in this experiment.

DOI: 10.1103/PhysRevC.65.044605 PACS number(s): 24.10.−i, 25.60.Dz, 27.20.+n, 29.25.Rm

I. INTRODUCTION

Secondary radioactive nuclear beams (RNBs) offer unique opportunities in the study of heavy-ion reactions [1–3]. Of interest in the present work is the production of *isomeric* secondary beams, in particular the metastable isomer $^{18}F^m$. Little is known about reactions involving metastable nuclei, yet such isomeric nuclei may play important roles in certain astrophysical processes. If their reaction cross sections are significantly different from those of the ground state, and if their lifetime is sufficiently long, such isomers may be important in explosive nucleosynthesis, rp processes, or astrophysical network calculations, for example.

Measurements on isomeric nuclei are in progress by our group and others. Studies of reactions involving radioactive beams and *targets* enriched with relatively long-lived metastable isotopes, such as $^{178}Hf^m$, have been reported [4–6].

Short-lived secondary isomeric beams may be identified by their γ decays. They have been used previously for reaction studies [7,8]. Here, secondary ''γ-tagged'' beams allow good isotopic separation and online measurement of the isotopic purity [7–10]. The identification and separation online were done in earlier experiments where our group produced a secondary $^{18}F^m$ beam, and measured $^{18}F^m + p$ elastic scattering [9] and the total reaction cross section, σ_R, on Si [10]. Recently, another experiment has been performed to measure Coulomb excitation and deexcitation by scattering $^{18}F^m$ on a gold target [11]. In the present experiment we have studied the behavior of nuclear reaction cross sections in silicon for the high-spin (5^+) isomeric nucleus $^{18}F^m$. An initial set of measurements indicated a rather strong low-energy enhancement in the total reaction cross section, σ_R, of $^{18}F^m + Si$ [10]. This earlier experiment was, however, not optimized for low-energy measurements. The data extracted for the lowest energies had considerable statistical uncertainties. The present experiment has significantly better statistics, and the detectors selected for use were better suited for measurement of reaction cross sections below 150 MeV.

Certain RNBs, particularly those with low valence-nucleon binding energies such as ^{11}Li, have been predicted to exhibit rather large enhancements in their σ_R at low energies including the region near the Coulomb barrier [12]. Most measurements involving stable and β-unstable nuclei, such as $^{6,7,8,9,11}Li$, were intended to determine high-energy ''interaction'' cross sections. These were deduced primarily from break-up reactions [1–3], or σ_R measured in one [13–18] or a few [13,19,20] relatively thick particle detectors where the detectors are used as ''active'' targets. While these measurements indicate an increase in σ_R with decreasing neutron binding energy, additional measurements are needed

to determine σ_R near the Coulomb barrier where projectile breakup may not be the dominant reaction mechanism. It is well known that excitation functions at low energies are sensitive to properties, such as the diffuseness, of the nuclear wave functions at the periphery of nuclei. Hence, measurements of excitation functions are particularly useful for the study of RNBs.

II. EXPERIMENTAL SETUP

In the present experiment, a secondary beam of the short-lived, high-spin, isomeric nucleus $^{18}F^m$ ($J^\pi = 5^+, E_x = 1.1$ MeV, $T_{1/2} = 162$ ns) was produced using a primary ^{17}O beam produced by the K1200 cyclotron at the National Superconducting Cyclotron Laboratory (NSCL) at Michigan State University. The $^{18}F^m$ was obtained using the selective, high-cross-section single-nucleon transfer reaction $^{17}O(^{12}C, ^{11}B)$ $^{18}F^m$ at a primary ^{17}O beam energy of 25 MeV/nucleon. The secondary $^{18}F^m$ ions, along with other ions such as $^{18}F_{g.s.}$, ^{14}N, $^{16,17,18}O$ were magnetically selected and brought to a secondary focus using the University of Michigan 7 T large-bore (0.4 m) superconducting solenoid [7] at NSCL-MSU. The solenoid acts as a simple ion-optical lens. It was configured with short object and image distances. We refer to this configuration as the short flight path mode, since the flight path from the production target to the secondary target is only about 3 m. This short flight path allows the transport of the secondary $^{18}F^m$ beam with minimum in-flight decay. In this mode the system produces an isotopic ^{18}F group, which is approximately 70% metastable and 30% in its ground state. The ground-state fraction is almost completely due to in-flight decay of the initial isomeric state. The ground and isomeric states are fully magnetically separated in the solenoid due to the 1.1 MeV excitation energy. Secondary beam intensities of approximately 10^4 particles per second are possible with primary ^{17}O beam intensities of a few particle nanoamperes. In the present experiment the rate of *all* ion groups in the detector stack was kept below 10^2 particles per second to reduce pileup in the detector system. The total rate of $^{18}F^m$ was approximately 2% of this rate, or approximately 5000–7000 $^{18}F^m$ per hour.

The solenoid is a strongly double-focusing device for ions near 0°. These ions are a good match to the solenoid, resulting in good optical properties of the secondary beam at the focus. The beam is focused with a spot size of a few mm^2, with a beam divergence less than $\pm 3°$ [9,10].

The isomer $^{18}F^m$ is in a *very*-high-spin state, $J^\pi = 5^+$. We note here that the ground-state spin and parity of $^{18}F_{g.s.}$ is $J^\pi = 1^+$. The energy level scheme of ^{18}F is shown in Fig. 1 [21]. The 5^+, 3^+, and 1^+ levels are members of the $\pi(d_{5/2})\nu(d_{5/2})$ two-nucleon multiplet coupled to the $J^\pi = 0^+$ ^{16}O core. The $^{18}F^m$ half-life (162 ns) is sufficiently long to allow transport of the beam to a secondary target, yet short enough to use fast particle-γ coincidence techniques to identify the subsequent isomer γ decays ($\gamma_1 = 182$ keV, $\gamma_2 = 937$ keV).

A version of techniques previously used by Brown *et. al.* [9,22] and Warner *et al.* [14,19,20] was developed to measure the σ_R as a function of energy. The newer method developed for the present experiment employs a ''stack'' of particle detectors [10,18–20] that permits simultaneous measurements at several energies.

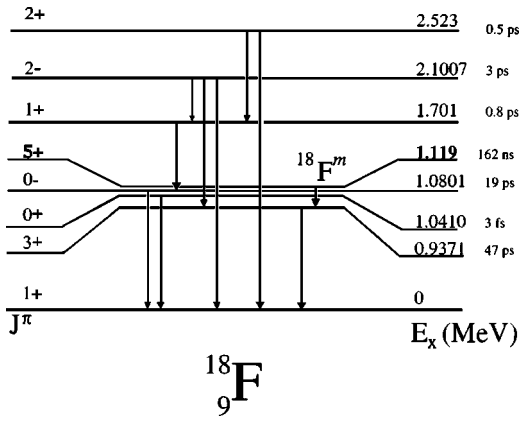

FIG. 1. ^{18}F nuclear level scheme. Spins and parities of the levels are shown on the left side, while the excitation energies and half lives are shown on the right side of the figure. The dominant decay mode of the 5^+ isomeric states is the cascade $5^+ \rightarrow 3^+ \rightarrow 1^+$.

Initially it was intended to use a stack of detectors as follows: a 100 μm silicon surface barrier (SiSB) detector, a 40 μm SiSB detector, a 200 μm boron implanted position sensitive (PSD) silicon detector, three 100 μm SiSB detectors, and a 1000 μm lithium drifted silicon [Si(Li)] detector. This would have left the beam energy $\approx$35–45 MeV incident on the sixth detector, very near the Coulomb barrier. The 40 μm detector was replaced due to malfunction, first with a 200 μm detector and then finally with a 74 μm SiSB detector. This left the final incident energy at the fifth detector approximately 50 MeV above the Coulomb barrier.

The detectors were placed in a linear stack, centered on the beam axis. The seven detectors were packed as closely as practical. The detector stack was 8 cm long, with an average distance between adjacent detectors of approximately 1 cm. In the first experiment [10] a CsI crystal attached to a *p-i-n* diode was placed behind the seven surface barrier detectors as a detector for light ions from breakup events of ^{18}F, such as $^{18}F \rightarrow {}^{16}O + d$, and γ rays. Unfortunately, the CsI detector was not successful in this mode, due to the large neutron and γ-ray fluxes associated with the production of the $^{18}F^m$ at the front of BigSol, and the slow decay time of the signal from CsI crystal and the *p-i-n* diode combination. The neutrons from the production target are numerous at 0°, and the solenoid refocuses the secondary beam to 0°. In this configuration one cannot swing the secondary beam away from 0°, as is possible in more conventional analysis systems, such as the A1200 channel at NSCL-MSU. For the present experiment, the CsI detector was replaced with a thick Si(Li) detector. Use of the Si(Li) detector also proved unsuccessful in detecting these breakup reactions, again due to the high fluxes of neutrons, γ rays, and light ions present in the secondary beam. The extended temporal length of the energy pulse from the Si(Li) detector was also a factor. A very fast detector, such as a plastic scintillator, with good γ ray efficiency is needed for this purpose in the future, but has not yet been used.

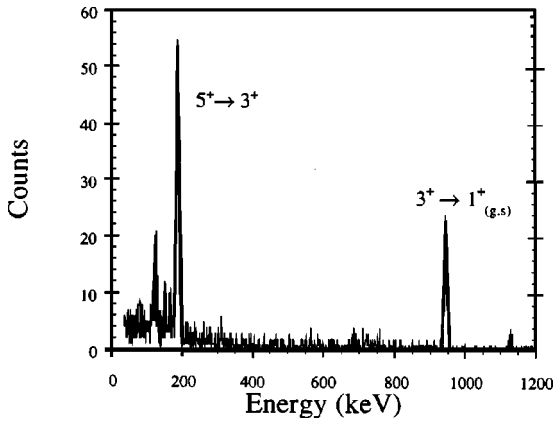

FIG. 2. γ-ray energy spectrum from the HPGe detector of events identified as ^{18}F ions in the particle detector stack.

A calibrated hyperpure germanium (HPGe) γ-ray detector was placed outside the scattering chamber 15 cm from the center of the silicon detector stack. This detector served as the primary detector for $^{18}F^{m}$ γ rays [9,10]. The HPGe detector also served to accomplish the final tuning of the current in the solenoid. The required solenoid current was estimated by using a ray tracing code developed by our group [22,23]. The current determined by this calculation was accurate to 1%. The magnet was initially set to the estimated current given by this ray tracing code. The current in the solenoid was then adjusted from the initial setting to produce the maximum rate of $^{18}F^{m}$ at the PSD in the detector stack. This final current tuning was accomplished by identifying ^{18}F in the silicon detector stack, and maximizing the ratio of the sum of the events in the two $^{18}F^{m}$ γ-ray peaks, 182 keV and 937 keV, from the HPGe detector, relative to the number of ^{18}F identified in the silicon detector stack. Figure 2 shows such a γ-ray spectrum, software gated by ^{18}F events identified in the silicon detector stack. From this measurement the intensity of the secondary beam and the isotopic and isomeric purity were determined.

Furthermore, the HPGe detector was used online to monitor the rate of $^{18}F^{m}$ incident on the detector stack. Any time the ratio of the number of $^{18}F^{m}$ γ rays detected by the HPGe detector to ^{18}F particles identified in the silicon stack varied by more than 5% the experiment was halted, and the solenoid magnet current was adjusted. This is necessary since a primary beam energy shift of 0.3% would defocus the isomeric state from the silicon detector stack, yet would continue to deliver $^{18}F_{g.s.}$. Conversely, the $^{18}F_{g.s.}$ ions could also be focused onto the detector telescope by a small increase in the solenoid current; this defocuses the $^{18}F^{m}$ leaving primarily ground-state ions. Defocusing due to fluctuations in the supply current seems not to be a problem though, largely due to the large reactance of the solenoid-power supply system, and the stability of the power supply. It is obvious, from the discussion above, that the calibration, in energy and efficiency, of the HPGe detector was critical. The fraction of the ^{18}F in the metastable state, determined by the HPGe detector, was used to unfold σ_R of the metastable state from the measured mixed state $(\sigma_R)_{\text{mixed}}$ and measured ground state $(\sigma_R)_{\text{g.s.}}$.

The energy and efficiency calibrations of the HPGe were both accomplished using a standard reference material (SRM) calibrated γ-ray source developed by, and obtained from, the National Institute of Standards and Technology (NIST) [24]. The source is described as follows (from the documentation supplied with the source): ''Sample consists of a dried deposit of radionuclides between two layers of polyester type 0.006 cm thick which are mounted on an aluminum annulus (3.8-cm inside diameter and 5.4-cm outside diameter).'' There are 18 distinct γ-ray lines emmitted by the source, which vary from an energy of 27 keV to 1596 keV. The uncertainty in the emission rate of each of these lines is typically 1% or less. These lines are from ^{126}Sb, ^{154}Eu, or ^{155}Eu. The initial emission rate of each of these γ-ray lines as of 1200 EST, September 1, 1988 was supplied by NIST. The half-lives of each of the source isotopes are well known [24]. The energy calibration of the HPGe detector was accomplished via a typical linear regression of the channel number versus the energies given by the NIST documentation. The efficiency calibration was more difficult because the ^{18}F may stop in different detectors depending on the range of the ^{18}F and the configuration of the detector stack. Thus it was necessary to calibrate the HPGe detector for each possible position at which the ^{18}F secondary beam might stop, and then choose the correct efficiency over the range of the ions and the configuration of the detector stack.

Seven separate efficiency calibrations of the HPGe detector were performed. These calibrations were done with the NIST source at the front of the first detector, and between each two adjacent detectors. Each of these positions for the NIST source only approximated the position at which the secondary beam would actually stop within the detector stack. Thus it was necessary to interpolate the efficiency for the actual range of the secondary beam. Each of these steps was straightforward, but had to be done with great care. The actual efficiency at a given energy was measured by integrating the counts within a γ-ray peak, and dividing by the known emission rate corrected for the decay since September 1, 1988. The efficiency was further corrected for the dead time of the detector and data acquisition system. The area under each peak was found from fitting the peak with a Gaussian curve. Background was estimated by a polynomial fit of the background in the immediate vicinity of each peak. The total error for each peak was determined by adding in quadrature the uncertainties from the area under the peaks, the areas of the backgrounds, the dead time correction, and the predicted emission rates from the NIST source.

The experiment was run in two parts: first, the secondary beam, containing the mixed ground and isomeric states, was focused on the detector stack by adjusting the current in the solenoid to maximize the yield of isomeric-state γ rays in the HPGe; second, the solenoid current was adjusted to defocus the isomeric state, leaving primarily ground-state ions in the secondary beam. This was necessary since the isomeric secondary beam had ground-state contamination due to the in-flight decays of the isomeric state, and from the rather large momentum bite of the solenoid, $\Delta P/P \approx 3\%$. For the mixed-state beam it was necessary to measure the fraction of the ^{18}F ions collected that are in the isomeric state at the detector

location, i.e., the isomeric purity, α, of the mixed-state beam. The measurement of α was done with the HPGe detector. The σ_R were measured for both the ground- and mixed-state beams. Using α and the measured σ_R for the mixed and ground states we extracted the σ_R of the isomeric state.

The secondary beam, which includes all ions sharing the same magnetic rigidity, was reduced to an intensity of about 100–200 particles per second, of which approximately 2% were ^{18}F. This rate was chosen to allow reasonable statistics, without excessive pileup. In principle, the γ-ray decays from the $^{18}F^m$ could be measured in coincidence. However, the HPGe detector *total efficiency*, including the solid angle and the intrinsic efficiency of the detector, was less than 1%. Thus, measurement of γ rays from reaction events yielded too few events to identify any specific final states. By monitoring the γ rays from the isomeric state, we were able to track, and correct, drifts in any ''upstream'' beam line components that may have affected the energy or stability of the primary ^{17}O beam. This allowed us to improve, by nearly 30%, the energy spread in the secondary beam relative to the unmonitored secondary beam energy of the previous experiments [9,10]. Such long-term beam-energy stability is important in this type of measurement where we must extract data near other, intense, ion groups.

For each event the parameters acquired consisted of the energy signal and timing signal for each detector. The in-house data acquisition system of NSCL was used. The data were recorded on 8 mm tape for later offline analysis.

III. DATA ANALYSIS

The technique used in this experiment is closely related to the conventional ''attenuation'' method of measuring σ_R. In this case individual incident ions are tracked through the ''target,'' here the silicon detectors in the detector telescope. The ''missing'' ions due to nuclear reactions are identified by observing the energy loss in each detector.

During analysis of the data, a software gate was applied to the reconstructed position in the position sensitive detector (PSD) detector to ensure that only particles that are on, or near, focus were accepted. This focus of the isomeric-state particles separates them well from the off focus ground-state contamination. Also, the ions are well displaced from the edges of the detector, and thus are unlikely to have scattered from the physical apertures of the system or to be scattered out of the detector stack. One-dimensional (1D) gates were placed on timing signals between each surface barrier detector and the cyclotron rf time of flight (TOF). This ensured that the energy signal from each detector came from the same beam burst of the cyclotron, and that all the energy signals were well correlated in time. Furthermore, a two-dimensional (2D) software gate was placed on the particle identification (PID) spectra of the energy loss versus the TOF signal of the first detector (ΔE_1-TOF$_1$). The cut on ΔE_1-TOF$_1$ selected the ion species of interest from the surrounding ion groups, albeit with a small amount of contamination from other ion species. The last 2D gate used was applied to ΔE_1 versus the sum of energy deposited in all of the detectors, E_{total}. This gate was needed to eliminate contamination, due to straggling in the first detector, from neighboring ions, such as ^{20}Ne, ^{16}O, and ^{17}O.

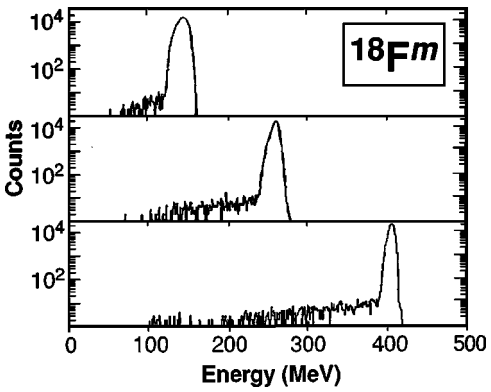

FIG. 3. Energy spectra for ^{18}F in three different detectors in the detector stack. The counts in the low-energy tails below the peak represent reactions of the ^{18}F with Si in the detectors. There are also unidentified reactions $Q \approx 0$ under the peak as well.

The energy signals that passed the analysis described above represented the energy-loss history of the chosen ion in the detector stack. A set of seven summed energy signals was formed:

$$E_{j,7} = \sum_{i=j}^{7} \Delta E_i , \tag{1}$$

for instance $E_{4,7} = \Delta E_4 + \Delta E_5 + \Delta E_6 + \Delta E_7$. Obviously, $E_{1,7}$ is the total energy lost by an ion in the detector stack.

A further set of six 2D spectra were incremented, ΔE_i versus $E_{(i+1),7}$; for example, ΔE_2 versus $E_{3,7}$. Each of these spectra shows a horizontal band of events extending from the central, noninteracting peak [16,17]. This horizontal band contains the energies of all metastable ions, including those which have reacted in the detectors. A rectangular 2D reaction identification gate (RID) is placed around this horizontal band and the central peak in each of these spectra. Figure 3 shows 1D energy spectra for detectors 1–7 (bottom), 3–7 (middle), and 5–7 (top), which have passed the respective RID gate. With this analysis it was possible to measure the σ_R for separate energies.

In these 1D energy spectra the events within the main peak are either unreacted, elastically scattered, or reacted with small Q values. The counts outside the peak, plus an extrapolated estimate of the number of low Q value reactions within the peak, were summed and used to calculate the reaction probability. The reaction probability is defined as

$$P(E) = \frac{N_{\text{reactions}}}{N_{\text{total}}}, \tag{2}$$

where $N_{\text{reactions}}$ is the number of reaction events, N_{total} is the total number of events, and E is the incident energy of the ions [10,17–20]. The reaction probability is related to the reaction cross section as follows:

$$1 - P(E) = \exp\left[-\nu \int_0^E \left(\frac{\sigma}{S} \right) dE' \right], \tag{3}$$

where ν is Avagadro's number multiplied by the density and divided by the atomic number of the target material, σ is the reaction cross section, and S is the stopping power dE/dx. We define the average reaction cross section between two incident energies E_1 and E_2 as

$$\overline{\sigma} = \int_{E_1}^{E_2} \frac{\sigma}{S} dE' \Big/ \int_{E_1}^{E_2} \frac{1}{S} dE'. \tag{4}$$

It is easily shown then that the average cross section for a particle incident on a detector with an energy E_2 and exiting the detector with energy E_1 in terms of the reaction probabilities is

$$\overline{\sigma}_R = \ln\left(\frac{1-P(E_2)}{1-P(E_1)}\right) \Big/ \nu \int_{E_1}^{E_2} \frac{1}{S} dE'. \tag{5}$$

Based on measurements using other beams [14,15,17–20] the uncertainty of the estimate of $Q \approx 0$ reactions, typically 4% or less that all the reaction events, was assigned to be 50%. This uncertainty was added in quadrature to the other statistical uncertainties.

Unlike other reaction cross-section measurements [1–3], such as γ-ray detection or measurement of individual fragments, the technique described above does not require knowledge of the multiplicity of the reaction event. One only needs to know that the total energy of the detected reaction products is different from that of other, nonreacting particles of the same ion species. The only difficulty in this method, as discussed above, is the estimate of nonelastic reactions with $Q \approx 0$. The latter method may underestimate the cross sections for unstable nuclei, since these can have reactions with $Q \geqslant 0$ but are not identified [25]. Most elastic scattering events will still properly identify as $Q=0$ events provided the detectors are large relative to the incident beam spot, as is the case in this experiment, so that elastically scattered particles are not scattered out of the detector telescope. For this experiment, the scattered projectile and the recoil Si ion are detected as a single event with the summed energies in the SiSB detectors, disregarding the small pulse-height defect of the heavier Si recoil. Thus the reaction cross sections deduced here are *inelastic* nuclear reactions, and the *elastic* scattering contribution is excluded from these measurements.

The ^{18}F beam incident upon the stack includes some nuclei in the ground state that have decayed during the 56 ns time of flight from the production target to the detector stack. Using the calibrated HPGe detector we accurately measured α of the ^{18}F beam at the detector stack [8]. In this experiment, as in our previous measurements [10], α is approximately 70%±2%. Knowing the value of α for the beam, and measuring the σ_R of the ground-state and the mixed-state beam, we can extract the reaction cross section for the isomeric state as

$$\sigma_{\text{isomeric}} = \frac{1}{\alpha}\sigma_{\text{mixed}} - \frac{1-\alpha}{\alpha}\sigma_{\text{ground state}}. \tag{6}$$

Here σ_{mixed} and $\sigma_{\text{ground state}}$ are the measured cross sections for the mixed and ground-state beams, respectively. Above 300 MeV we conclude that the cross sections for the ground and isomeric states are nearly equal, since the measured cross sections for the isomeric-state and the mixed-state beams are nearly equal [10].

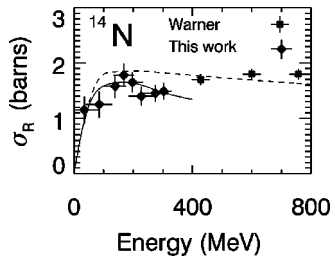

FIG. 4. Measured reaction cross sections for ^{14}N from this experiment and from Warner *et al.* [13]. An OM calculation, with parameters given in Table I, is shown by the lower solid line, the upper line is a Glauber calculation.

IV. EXPERIMENTAL RESULTS

Data were collected on the stable nuclei ^{14}N and ^{16}O simultaneously with ^{18}F. The same data analysis procedure was used on these ion species as for the ^{18}F. Measuring the cross sections of both ^{14}N and ^{16}O allows us to compare the analysis with this multidetector particle telescope with data taken in previous experiments using a two-detector stack.

The assigned energies are the averages of the incident and exit energies of the ions of interest passing through each detector. The uncertainties in energy for each data point are assigned from the average incident energy to the average exit energy of the ion of interest in each detector.

Figure 4 shows the data for ^{14}N and an optical model (OM) calculation using the parameters shown in Table I. Likewise, Fig. 5 shows our data and an OM calculation for

TABLE I. Optical model (OM) parameters used in Figs. 6–8.

Ion species	V_R (MeV)	a_R (fm)	R_R (fm)	W_I (MeV)	a_I (fm)	R_I (fm)	V_{so} (MeV)	R_C (fm)
^{14}N	$-41.8-0.019\,E$	0.5	7.08	$-12.9+0.0188\,E$	0.5	7.08	0.0	6.81
^{16}O	$-42.5-0.017\,E$	0.5	7.23	$-13.0+0.0192\,E$	0.5	7.23	0.0	6.95
^{18}F$_{\text{g.s.}}$	$-43.3-0.017\,E$	0.5	7.36	$-12.3+0.0181\,E$	0.5	7.36	0.0	7.07
^{18}F^m	$-40.5-0.014\,E$	0.8	7.36	$-11.5+0.0177\,E$	0.8	7.36	0.0	7.07

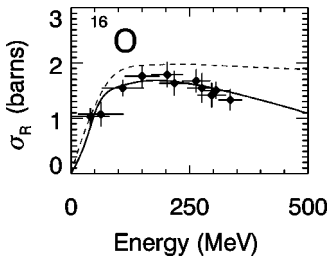

FIG. 5. Measured reaction cross sections for ^{16}O. An OM calculation is shown by the lower line, with parameters given in Table I. The upper line is a Glauber calculation.

^{16}O. The parameters used in the OM calculation are again shown in Table I. These data agree well with the optical model calculations shown in the figures, except for the ^{14}N data above 400 MeV given by Warner *et. al.* [16], which does not show the expected fall off predicted by our OM calculations.

Figure 6 shows the total nuclear reaction cross sections measured for $^{18}F_{g.s.}$, Also shown is an OM calculation, where the parameters for the fit are given in Table I. Figure 7 shows the extracted reaction cross sections for $^{18}F^{m}$. The upper curve in the figure is an OM calculation using the parameters given in Table I. The middle curve in Fig. 7 represents OM calculation shown in Fig. 6 for the ground-state data.

The cross sections for $^{18}F^{m}$ are larger than for $^{18}F_{g.s}$. This feature is particularly striking when comparing the low-energy behavior. The difference between the cross sections for the isomeric and ground states has a maximum in the range of 100 to 200 MeV. At laboratory energies near 200 MeV the $(\sigma_R)_{\text{isomeric}}$ appears to be enhanced compared to $(\sigma_R)_{\text{g.s.}}$ by about 30% as seen in Fig 8. Figure 8 shows the ratio of the OM fits for the isomeric state and the ground state. Below 100 MeV only one data point for the ground state and one data point for the isomeric state have been measured; for this reason the values for the ratio of the isomeric state to the ground state below 100 MeV should not be considered reliable. We note that while the maximum ehancement is approximately 30%, the *average* enhancement from 100 MeV to 450 MeV is 18%.

Our earlier measurements for $^{18}F^{m}+$Si seemed to indicate an even larger enhancement of the cross sections at the lowest energies [10] but was limited by statistical and other uncertainties. The present experiment, with a detector stack

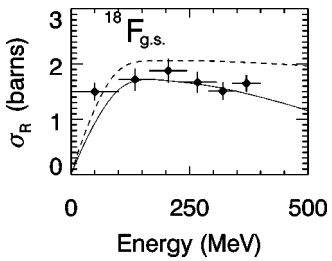

FIG. 6. Measured reaction cross sections for $^{18}F_{g.s.}$. The lower line is an OM calculation, with the parameters described in the text and given in Table I. The upper line is a Glauber calculation.

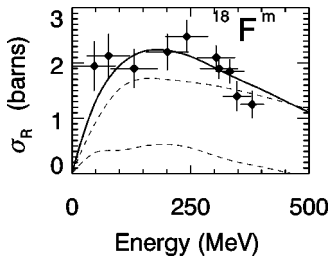

FIG. 7. Measured reaction cross sections for $^{18}F^{m}$. The upper line is an OM calculation for the metastable state, with the parameters described in the the text and given in Table I. The middle line is the OM calculation for the ground state shown in Fig. 6. The lower line is the difference between the OM calculations for the metastable state and the ground state.

better suited for the low-energy measurements and significantly better statistics, still indicates a sizable and statistically significant enhancement of $(\sigma_r)_{\text{isomeric}}$.

V. DISCUSSION OF RESULTS

We have found an enhancement of the reaction cross section, for the isomer $^{18}F^{m}$ over the cross sections for $^{18}F_{g.s.}$. Above 300 MeV, the isomeric and ground states appear to have essentially equal reaction cross sections. The isomeric- and ground-state reaction cross sections above 300 MeV have behavior similar to other nearby stable nuclei. From reaction studies of ^{16}O(α,d), ^{17}O(α,t) [26], and from the reaction used as our production reaction, ^{12}C(^{17}O,^{18}F)^{11}B [27], the basic nuclear structure of both $^{18}F_{g.s.}$ and $^{18}F^{m}$ appears to be understood. A simple model of ^{18}F consists of an ^{16}O core with the last proton and neutron being "valence" particles which are coupled to form a $J^{\pi}=1^{+},3^{+},5^{+}$ $(\pi d_{5/2})$ ν $(d_{5]/2})$ multiplet. For the ground state, with $J^{\pi}=1^{+}$, the valence proton and neutron are in counterrotating orbits with poor spatial overlap. On the other hand, the isomeric state, with $J^{\pi}=5^{+}$, is highly correlated, and may be thought of as a deuteron $(S=1)$ state, bound in an ^{16}O potential with $L_d=4$. Evidence for this structure comes from the reaction ^{16}O(α,d)^{18}F where the isomeric level is found to be preferentially populated in the deuteron transfer [26]. It seems likely that this highly correlated nature of the valence proton and neutron leads to the enhanced cross sections at low en-

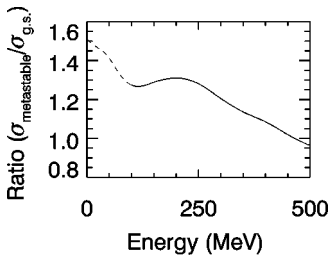

FIG. 8. Ratio of reaction cross sections for $^{18}F^{m}$ and $^{18}F_{g.s.}$. The values below 100 MeV are extrapolated from the data and should not be considered reliable. A maximum enhancement of the reaction cross section of approximately 30% is seen at 200 MeV. The average enhancement in the range 100 to 500 MeV is 18%.

ergies found in the present work. One may include the above feature in $\sigma_R(E)$ calculations using a Glauber model approach [26–29].

Calculation of $\sigma_R(E)$ at low energies, can be done using the nuclear optical model (OM). The OM potential, in turn, can be related to the matter density of the nuclei involved through the use of the folding optical model (FOM) [30,31]. For heavy ions, the FOM involves a double folding procedure [32,33]. It will be sufficient for our purpose to use the conventional optical model, deduce the appropriate OM potential parameters, and relate these to the corresponding FOM parameters, such as mean square radii $\langle r^2 \rangle$ and OM potential volume integrals [30–33].

In Figs. 4–7 optical model calculations are shown for the ^{14}N, ^{16}O, $^{18}F_{g.s.}$, and $^{18}F^m$. The starting parameters for these calculations were adopted from a ''global'' OM set, determined from low-energy elastic scattering of oxygen and other ions, from a series of targets in the mass range $A=40$ to $A=90$. Table I shows the parameters used in these OM calculations. The upper curves in Figs. 4–6 are Glauber calculations.

In the parameter set shown in Table I the following interaction radii are calculated as

$$R_R = 1.30(A_1^{1/3} + A_2^{1/3}) \text{ fm}, \tag{7}$$

$$R_I = 1.30(A_1^{1/3} + A_2^{1/3}) \text{ fm}, \tag{8}$$

$$R_C = 1.25(A_1^{1/3} + A_2^{1/3}) \text{ fm}. \tag{9}$$

As is well known, the nuclear interaction is reduced at high energies and requires an energy-dependent optical model [32]. Therefore a suitable energy dependence was introduced into the potentials V_R and W_I, as indicated in the table, where E is the laboratory kinetic energy of the projectile ion.

In order to reproduce the magnitude and energy dependence of the $^{18}F^m$ data, we needed only to increase the diffuseness of the optical potentials, a_R and a_I, from 0.5 fm to 0.8 fm with a corresponding lowering of V_R and W_I. These changes keep the total volume integral of the real and absorptive potentials roughly the same, yet increase the radial extent of V_R(r) and W_I(r). Specifically, the mean square radius, $\langle r^2 \rangle$ of the $^{18}F^m$+Si optical potential is approximately 5 fm^2 larger then that of $^{18}F_{g.s.}$+Si. This provides the needed enhancement for $^{18}F^m$ at low energies, while ensuring that the high-energy behavior remains, basically, unaffected. Changes in other parameters were unnecessary given the good fit obtained simply by adjusting a_I and a_R. This might be expected given the classical Coulomb dominated orbits of the ions at low collision energies. For these low energies $\sigma_R(E)$ is primarily determined by the ''tail'' of the OM potentials, and in particular by W_I(r) [26].

The valence-nucleon structure of a heavy ion can result in large enhancements of fusion cross sections, even for stable nuclei well below the Coulomb barrier. In this work, a similar enhancement appears to occur from near the Coulomb barrier up to approximately 300 MeV for the isomeric state of fluorine. If one considers a model of the $^{18}F^m$ as a deuteron, with high angular momentum, orbiting an ^{16}O core, then it seems reasonable to assume that the enhancement seen in the data may be due to this correlated proton-neutron pair that acts as a valence ''deuteron.'' Since the enhancement is seen in neither the ^{14}N nor ^{16}O data, the assumption that the correlated proton-neutron pair in the $^{18}F^m$ is a key factor in the enhancement of the reaction cross sections would seem reasonable. This assumption is further supported by the fact that the low-spin (1^+) ground state of the ^{18}F shows no enhancement of this reaction cross section at the same energies.

We consider a more quantitative comparison. The optical model represents a convolution, or ''folding,'' of the nucleon-nucleon interaction with the nucleon distributions of both the target and projectile nuclei. We compare the $\delta\langle r^2 \rangle$ of the optical model potentials that were necessary to fit the cross-section data to a corresponding change in the nucleon distribution when going from the ground-state configuration of fluorine to the metastable configuration, $^{18}F_{g.s.} \rightarrow {}^{18}F^m$. The shift $\delta\langle r^2 \rangle_{OM} \approx 5$ fm^2 as a_r and a_I increase from 0.5 fm to 0.8 fm using a Wood-Saxon form, as the fluorine configuration goes from the ground state to the metastable state. The corresponding $\delta\langle r^2 \rangle$ of the nucleon distribution of $^{18}F_{g.s.}$ ($J^\pi = 1^+$) to $^{18}F^m$ ($J^\pi = 5^+$) can be calculated by considering $^{18}F^m$ in a cluster model as an $^{16}O_{g.s.}$ ($J^\pi = 0^+$) core plus a valence deuteron ($S=1$) with $L_d = 4$ and the appropriate deuteron binding energy. Using a harmonic oscillator or a Wood-Saxon potential and taking an appropriate weighting of nucleons in $^{18}F_{g.s.}$ and $^{18}F^m$ yields $\delta\langle r^2 \rangle_{c.m.} \approx 0.5$ or 1.0 fm^2, respectively, for the two potentials. This value is less than the value observed for $\delta\langle r^2 \rangle_{OM}$ derived from the data. This indicates that while a simple cluster model of the metastable state is in qualitative agreement with the experiment, it is inadequate to calculate the reaction cross sections measured in the present work.

Although we have included a linear energy-dependent term in the OM calculation, this term is derived from OM fits to relatively low-energy data and is likely not accurate at higher energies. The Glauber model calculations, on the other hand, are derived from known nucleon-nucleon cross sections and are more appropriate at higher energies. This may explain the differences between the OM calculations and Glauber calculations shown in Figs. 4–7.

Finally, it should be noted that the enhancement seen for $^{18}F^m$ is comparable to the enhancements seen for some of the neutron and proton ''halo'' nuclei [20]. The enhancements for these halo nuclei are typically seen at higher energies where a Glauber model may be used. It is possible, given the results reported here, that these larger cross sections may be due to an increased diffuseness parameter in the equivalent optical model potentials for the halo nuclei.

VI. CONCLUSIONS

The present studies indicate an enhancement of the total nuclear reaction cross section for the $J^\pi = 5^+$ isomeric

nucleus $^{18}F^{m}$ on silicon at low energies. This enhancement is well reproduced by increasing the diffuseness of the conventional heavy-ion optical potential. We attribute the enhancement of these cross sections to the nature of the proton-neutron pair in the isomeric state, where the pair is in a highly correlated, high-spin state with a moderate binding energy. These measurements further demonstrate the feasibility of using isomeric nuclei for nuclear reaction studies. Furthermore, such studies may well uncover some interesting physics that may need to be considered in other contexts, such as astrophysical calculations.

ACKNOWLEDGMENTS

The authors wish to thank J. Bajema, J. J. Kolata, K. Lamkin, A. Nadasen, B. Sherrill, and the staff at NSCL-MSU for their assistance. This work was supported in part by the U.S. National Science Foundation under Contract Nos. PHY-8913815, PHY-9122067, PHY-9208468, PHY-9214992, and PHY-9804869 and the Nederlandse Orgnisatie voor Wetenschappelijk Onderzoek (NWO). The University of Michigan 7 Tesla solenoid magnet was funded under DOE Contract No. DE-FG02-88er75445 (DOE University Instrumentation Program).

[1] *Proceedings of the Second International Conference on Radioactive Nuclear Beams, Louvain-la-Neuve, Belgium, 1991*, edited by J. Vervier (IOP, Bristol, England, 1991).

[2] *Proceedings of the Third International Conference on Radioactive Nuclear Beams, East Lansing, 1993*, edited by D.J. Morrisey (Editions Frontiéres, Gif-sur-Yvette, France, 1993).

[3] *Proceedings of the Fourth International Conference on Radioactive Nuclear Beams, Omiya, Japan June 1996*, edited by S. Kubono, T. Kobayashi, and I. Tanihata [Nucl. Phys. **A616**, 1 (1997)].

[4] I.A. Kondurov, E.M. Korotikikh, Yu.V. Petrov, and G.I. Shuljak, Phys. Lett. **106B**, 383 (1981).

[5] H.J. Wollersheim, in *Future Directions in Nuclear Physics with 4π Gamma Detection Systems of the New Generation*, edited by J. Dudek and B. Haas, AIP Conf. Proc. No. 259 (AIP, New York, 1992).

[6] G. Rotbard, G. Berrier-Ronsin, O. Constantinescu, S. Fortier, S. Gales, M. Hussonnois, J.B. Kim, J.M. Maison, L-H. Rosier, J. Vernotte, Ch. Briancon, R. Kulessa, Yu.Ts. Oganessian, and S.A. Karamian Phys. Rev. C **48**, R2148 (1993)

[7] F.D. Becchetti, K. Ashktorab, J.A. Brown, J.W. Jänecke, D.A. Roberts, J. van Klinken, W.Z. Liu, J.J. Kolata, K. Lamkin, R.J. Smith, and R.E. Warner, Phys. Rev. C **42**, R801 (1990).

[8] F.D. Becchetti, J. Bajema, J.A. Brown, F. Brunner, H. Griffin, J.W. Jänecke, T.W. O'Donnell, R.S. Raymond, D.A. Roberts, R.S. Tickle, R.M. Ronningen, H. Laumer, N. Orr, and A. Zeller, Nucl. Instrum. Methods Phys. Res. B **79**, 326 (1993).

[9] J.A. Brown *et al.*, in Ref. [1], p. 45; J.A. Brown *et al.*, in Ref. [2], p. 317; J.A. Brown, F.D. Becchetti, J. Jänecke, D.A. Roberts, D.W. Litzenberg, T.W. O'Donnell, R.E. Warner, N.A. Orr, and R.M. Ronningen, Phys. Rev. C **51**, 1312 (1995).

[10] D.A. Roberts, F.D. Becchetti, J.A. Brown, J. Jänecke, K. Pham, T.W. O'Donnell, R.E. Warner, R.M. Ronningen, and H.W. Wilschut, in *Proceedings of the International Symposium on Physics of Unstable Nuclei, Nigata, Japan, 1994*, edited by H. Horiuchi, K. Ikeda, K. Sato, Y. Suzuki, and I. Tanihata [Nucl. Phys. **A588**, 247c (1995)].

[11] J.A. Zimmerman, Ph.D. thesis, University of Michigan (2000).

[12] N. Takigawa, H. Sagawa, and T. Shinozuka, Nucl. Phys. **A538**, 221c (1992).

[13] R.E Warner, J.H. Kelley, P. Zecher, F.D. Becchetti, J.A. Brown, C.L. Carpenter, A. Galonsky, J. Kruse, A. Muthukrishman, A. Nadasen, R.M. Ronningen, P. Schwandt, B.M. Sherrill, J. Wang, and J.S. Winfield, Phys. Rev. C **52**, R1166 (1995).

[14] R.E. Warner, H.W. Wilschut, W.F. Rulla, and G.N. Felder, Phys. Rev. C **43**, 1313 (1991).

[15] R.E. Warner, C.L. Carpenter, J.M. Fetter, W.F. Waite, H.W. Wilschut, and J.M. Hoogduin, Phys. Rev. C **48**, 245 (1993).

[16] R.E. Warner, A.M. van den Berg, K.M. Berland, J.D. Hinnefeld, Z. Zhang, Y.T. Zhu, X.Q. Hu, and S. Li, Phys. Rev. C **40**, 2473 (1989).

[17] R.E. Warner, K.M. Berland, W.R. Rulla, D.A. Francis, J.J. Kolata, Z. Ayer, S.E. Darden, X.J. Kong, G. Liu, A. Morsad, S. McGimpsey, A.A. Rollefson, A. Galonsky, A. Nadasen, J.S. Winefield, and F.D. Becchetti, Nucl. Phys. **A516**, 416 (1990).

[18] R.E. Warner, C.P. Browne, S.E. Darden, J.J. Kolata, A. Rollefson, P.A. Kimoto, and A. Galonsky, Phys. Rev. C **37**, 1884 (1988).

[19] R.E. Warner, R.A. Patty, P.M. Voyles, A. Nadasen, F.D. Becchetti, J.A. Brown, H. Esbensen, A. Galonsky, J.J. Kolata, M.Y. Lee, R.M. Ronningen, P. Schwandt, J. vonSchwarzenberg, B.M. Sherrill, K. Subotic, J. Wang, and P. Zecher, Phys. Rev. C **54**, 1700 (1996).

[20] R.E. Warner, M.H. McKinnon, N.C. Shaner, F.D. Becchetti, A. Nadasen, D.A. Roberts, J.A. Brown, A. Galonsky, J.J. Kolota, R.M. Ronningen, M. Steiner, and K. Subotic Phys. Rev. C **62**, 024608 (2000).

[21] R.B. Firestone, V.S. Shirley, C.M. Baglin, S.Y. Frank Chu, and J. Zipkin, *Table of Isotopes*, 8th ed. (Wiley, New Work, 1996).

[22] J.A. Brown, Ph.D. thesis, University of Michigan, 1993.

[23] T.W. O'Donnell, Ph.D. thesis, University of Michigan, 2000.

[24] B.M. Coursey, D.D. Hoppes, and F.J. Schima, Nucl. Instrum. Methods Phys. Res. **193**, 1 (1982).

[25] W.Z. Liu, D.A. Roberts, J.W. Janecke, J.J. Kolata, A. Morsad, X.J. Kong, and R.E. Warner, Phys. Rev. C **40**, R1104 (1989).

[26] F.D. Becchetti, W.Z. Liu, K. Ashktorab, J.F. Bajema, J.A. Brown, J.W. Jänecke, D.A. Roberts, J.J. Kolata, K.L. Lamkin, A. Morsad, R.J. Smith, X.J. Kong, and R.E. Warner, Phys. Rev. C **48**, 308 (1993).

[27] E. Rivet, R. Phel, J. Cerny, and B.G. Harvey, Phys. Rev. **141**, 1021 (1966).

[28] R.E. Warner and G.N. Felder, Phys. Rev. C **42**, 2252 (1990).

[29] R.J. Glauber, *Lectures on Theoretical Physics* (Interscience, New York, 1959), Vol. I.

[30] S. Kox, A. Gamp, C. Perrin, J. Arvieux, R. Bertholet, J.F. Bruandet, M. Buenerd, R. Cherkaoui, A.J. Cole, Y. El-Masri, H. Longequeue, J. Menet, F. Merchez, and J.B. Viano, Phys. Rev. C **35**, 1678 (1987).

[31] G.W. Greenlees, G.J. Pyle, and Y.C. Tang, Phys. Rev. **171**, 1115 (1968).

[32] F.B. Becchetti and G.W. Greenlees, Phys. Rev. **182**, 1190 (1969).

[33] A. Nadasen, T. Steven, J. Farhat, J. Brusoe, P. Schwandt, J.S. Winefield, G. Yoo, N. Anantaraman, F.D. Becchetti, J. Brown, B. Hotz, J.W. Jänecke, D.A. Roberts, and R.E. Warner, Phys. Rev. C **47**, 674 (1993).